Uptake of NH_3 and NH_3 + HOBr Reaction on Ice Surfaces at 190 K

Ronghua Jin[†,‡] and Liang T. Chu[*,‡]

Department of Chemistry, Shanghai Normal University, Shanghai 200234, China, and Wadsworth Center, New York State Department of Health and Department of Environmental Health Sciences, State University of New York—Albany, P. O. Box 509, Albany, New York 12201-0509

Received: April 26, 2007; In Final Form: June 4, 2007

The uptake of NH_3 and the heterogeneous reaction of NH_3 + HOBr → products on ice surfaces at 190 K have been investigated in a flow reactor coupled with a differentially pumped quadrupole mass spectrometer. The uptake coefficient γ_t for NH_3 was determined to be $(3.8 \pm 1.4) \times 10^{-4}$ on ice films at 189.8 K, for a partial pressure of NH_3 in the range of 7.0×10^{-7} to 3.8×10^{-6} torr. The amount of NH_3 uptake on the ice film was determined to be $>2.9 \times 10^{15}$ molecules/cm^2, based on the total ice surface area at 189.2 K. The heterogeneous reaction of NH_3 + HOBr on ice surfaces has been studied at 190 K. The reaction probability γ_t was determined to be $(5.3 \pm 2.2) \times 10^{-4}$ and was found to vary insignificantly as HOBr surface coverage changes from 2.1×10^{13} to 2.1×10^{14} molecules/cm^2. A reaction pathway is proposed on the basis of experimental observations.

1. Introduction

Ice is one of the most abundant and important materials in the earth's environment. An understanding of the nature of the interaction of ice with its environment is important in an astrophysical context, because ice is a major component of comets, planetary rings, and interstellar clouds. Gas adsorption on icy surfaces is of interest in terrestrial, atmospheric, and interstellar chemistry.[1−4]

Ammonia in the atmosphere derives primarily from ground sources, including decaying organic matter and chemical fertilizers; the atmospheric lifetime is relatively short, ∼10 days, in the lower atmosphere.[5] Atmospheric NH_3 concentration varies significantly in both clean and polluted environments (50 pptv to 100 ppbv), as well as in cloud and fog droplets.[6−8] Current models for tropospheric aerosol growth depend on the condensation rates of ammonia, sulfuric acid, and water vapor.[9] Knowledge of the NH_3 uptake rate is important to an understanding of how NH_3 enhances new-particle nucleation rates beyond those observed for binary H_2SO_4−H_2O systems.[10−12] However, few studies have examined interactions between ice and NH_3 at tropospheric temperatures. NH_3 is arguably the most important alkaline atmospheric species.[6,13] Ammonium associated with aerosol particles exists well above the boundary layer. On average, rime ice samples are 50% neutralized by NH_3 uptake, and snow samples are on average 23% neutralized.[14]

Some related experimental and theoretical studies have been carried out on NH_3 adsorption at water interfaces[15−17] and on ice surfaces at low temperatures (typically <120 K).[18−24] The saturated coverage of NH_3 is $(1.2 \pm 0.2) \times 10^{14}$ molecules/cm^2 at the air−water interface at 298 K, and the NH_3 molecule is bound by a small number of water molecules at the surface.[15] The uptake coefficient for NH_3 at the water interface is $(9.7 \pm 0.9) \times 10^{-2}$ at $T = 290$ K.[17] Davidovits and co-workers show that the uptake coefficient of NH_3 on water has strong negative temperature dependence, increasing from 0.1 at 290 K to 0.3 at 260 K.[16,25] The interactions between NH_3 and H_2O molecules are weaker than those between HCl and H_2O molecules.[26]

NH_3 efficiently scavenges HOBr to form NH_2Br in the aqueous phase.[27] Halogenation of NH_3 has relevant roles in biochemistry and environmental chemistry.[28] Although the application of bromamines for drinking water disinfection was given serious consideration several decades ago, mainly because these chemicals were found to be stronger disinfectants than those chloramines, the brominated disinfection byproducts have relatively high genotoxicity and carcinogenicity.[29,30] Studies have been conducted on the reaction between NH_3 and HOBr in solution.[27,31−33] The specific rate constant for the NH_3 + HOBr reaction has been determined to be 7.5×10^7 M^{-1} s^{-1} at 20 °C.[31] Ice/snow is an important particulate matter in the lower atmosphere and at ground level, and atmospheric concentrations of NH_3 (∼0.2 ppbv in marine boundary layer[34]) and HOBr (∼0.01−0.26 ppbv[35]) are similar. A catalytic heterogeneous reaction usually has a reaction barrier that is lower than or equal to that of the corresponding noncatalytic reaction.[36] Presumably, the reaction between NH_3 and HOBr on ice surfaces is feasible in the lower atmosphere. Assuming that the reaction is rapid, it could serve to repartition bromine species and could constitute a potential sink for NH_3. To test this hypothesis, we have investigated the NH_3 reactive uptake by HOBr-treated ice surfaces.

The present study has been designed (1) to address the question of how rapidly NH_3 is taken up by the ice surface, under an NH_3 partial pressure comparable to pressures found in the atmosphere, and (2) to investigate the heterogeneous reaction of NH_3 with HOBr on ice surfaces at low temperature. In the following sections, we will briefly describe the experimental procedures used. We will present our determination of the initial uptake coefficient of NH_3 on ice surfaces, and the reaction probability of NH_3 on HOBr-treated ice surfaces, as a function of HOBr surface coverage. The results will be discussed in terms of a reaction mechanism.

2. Experimental Section

The uptake coefficient is defined as the ratio of the number of NH_3 molecules that are taken up by the ice surface to the

* To whom correspondence should be addressed. E-mail: lchu@albany.edu.
† Shanghai Normal University.
‡ State University of New York—Albany.

10.1021/jp073233m CCC: $37.00
Published on Web 07/26/2007

total number of NH_3 molecules colliding with that surface. When the ice surface is freshly prepared and the surface is clean, we term the uptake coefficient the initial uptake coefficient. When a reaction is involved, the reaction probability will be used. The measurements of both the uptake coefficient of NH_3 on ice and the reaction probability of NH_3 with HOBr-treated ice surfaces were performed in a flow reactor coupled with a differentially pumped quadrupole mass spectrometer (QMS). The details of the apparatus have been discussed in our previous publications;[37−39] we provide a brief summary and describe some modifications in the present paper.

2.1. Flow Reactor. The cylindrical flow reactor was made of Pyrex glass with an i.d. of 1.70 cm and a length of 35 cm. The outer jacket was a vacuum layer, so as to maintain the temperature of the reactor. The temperature of the reactor was regulated by a liquid-nitrogen-cooled methanol circulator (Neslab) and was measured with a pair of J-type thermocouples located in the middle and at the downstream end of the reactor. During the experiment, the temperature was maintained at 190 K; the stability of the temperature was better than ± 0.3 K in every experiment. The total pressure inside the flow reactor was controlled by a downstream throttle valve (model 651C, MKS Instruments) and was measured by a high-precision Baratron pressure gauge (model 690A, MKS Instruments). The stability of the pressure was better than 0.003 torr in every experiment. A double-capillary Pyrex injector was used to admit HOBr, He−water vapor, and NH_3 to the flow reactor. In order to avoid the condensation of the water vapor and reactants in the capillary at low temperature, room-temperature dry air was passed through the outside of the capillary, to keep it warm.

2.2. Ice-Film Preparation. The ice film was prepared by passage of helium carrier gas (99.9999% purity; BOC) through a high-purity distilled water (Millipore Milli-Q plus; >18 MΩ cm) reservoir. The reservoir was maintained at 293.15 ± 0.1 K by a refrigerated circulator (RTE-100LP, Neslab). Helium saturated with the water vapor was introduced to an inlet of the double-capillary injector. During the course of the ice deposition, the double-capillary injector was slowly pulled out, in a direction from the downstream end to the upstream end, at a constant speed, and a uniform ice film was deposited on the inner surface of the reactor at 190 K. The amount of ice substrate deposited on the wall surface of the flow reactor was calculated from the water vapor pressure, the mass flow rate of the helium−water mixture (which was measured by a Hasting mass flow meter), and the deposition time. The average film thickness, h, was calculated from the geometric area of the film on the flow reactor, the mass of the ice, and the bulk density ($\rho_b = 0.63$ g/cm^3) of vapor-deposited ice.[40] The typical ice-film thickness was approximately 3.5 ± 0.3 μm at 190 K.

2.3. NH_3−He Mixture. The NH_3−He mixture was prepared by mixing NH_3 (99.9%; Matheson) and helium (99.9999%; BOC) in an all-glass manifold, which had been previously been evacuated to ∼10^{-6} torr. The typical NH_3-to-He mixing ratio was 10^{-3} to 10^{-5}. The NH_3−He mixture, along with additional helium carrier gas, was introduced into the flow reactor via the glass and PFA tubing. The tubing was passivated by the NH_3−He mixture, to enable equilibrium to be established, as monitored by the QMS prior to every experiment. The amount of the NH_3−He mixture was controlled by two stainless steel needle valves in series, and the flow rate was determined from the pressure change in the manifold per minute. The relationship between the flow rate and NH_3 pressure change in the manifold was determined in a separate experiment. The typical pressure in the manifold was in a range of ∼250−600 torr, and the volume of the manifold was large (7 L). Pressure in the manifold changed by several Torr during an experiment. Therefore, we could maintain a constant flow rate during the experiment.

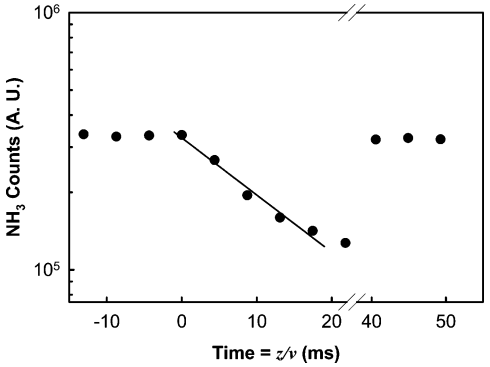

Figure 1. Plot of the log NH_3 signal vs the contact time (z/v) on ice at $P_{NH_3} = 1.9 \times 10^{-6}$ torr and 189.7 K. (●) represents the NH_3 signal. The plot shows the initial NH_3 signal, before the NH_3 came in contact with the ice ($t < 0$), the loss of NH_3 on the ice film ($t = 0-23$ ms), and the NH_3 signal after the NH_3 loss measurement. The injector was pushed back (a scale break indicates the data collection was paused) to the downstream end ($t \approx 40$ ms). The pseudo-first-order rate constant $k_{obs} = 58.1$ s^{-1} was determined using data recorded at $t = 0-17.5$ ms, and the corrected rate constant $k_w = 64.6$ s^{-1}. The initial uptake coefficient is $\gamma_w = 2.3 \times 10^{-3}$. The flow velocity was 9.4 m/s. The total pressure of the reactor was 0.500 ± 0.003 torr, and the background NH_3 signal was subtracted.

2.4. HOBr Preparation and Calibration. The HOBr solution was prepared by addition of bromine (99.5%; Aldrich) in aliquots to an ice-cooled glass flask, in which 2.1 g of $AgNO_3$ (99.9%, Baker) had been dissolved in 100 mL of distilled H_2O, until the orange color indicative of excess bromine persisted under continued stirring. After the solution had been stirred for ∼45 min, it was filtered to remove all precipitated AgBr. The filtered solution was freed of Br_2 by six successive extractions with CCl_4, each with 20 mL of CCl_4. A slightly yellowish, clear HOBr solution was obtained and was kept in a bubbler at 273.15 K in the dark.[41]

The concentration of HOBr vapor was calibrated by reaction of the HOBr vapor with HCl on ice surfaces at 190 K in a separate experiment, since the HCl concentration can be precisely controlled. The details have been given previously.[41,42]

2.5. Determination of the Uptake Coefficient. The initial uptake coefficient, γ_w, of NH_3 on the ice film was determined as follows. First, a 20 cm length of ice film was prepared by water vapor deposition on the inner wall of the flow reactor at 190 K, as described in section 2.2, for each separate determination. Second, the NH_3−He mixture was admitted to another inlet of the capillary injector. Before NH_3 was taken up by the ice film, the initial NH_3 signal was determined by the QMS (Figure 1, data at time $t < 0$). The loss of NH_3 was monitored by the QMS at $m/e = 16$, to minimize interference from the ice vapor. After the NH_3 signal was stabilized, the sliding injector was pulled out in 2 cm increments at a time, toward the upstream end of the flow reactor, to determine γ_w. The data acquisition time was typically ∼10−30 s/per point. The loss of NH_3 on the ice film was measured by the QMS, as a function of the injector distance z. For the pseudo-first-order loss rate under plug-flow conditions, the following equation holds for NH_3:

$$\ln[NH_3]_z = -k_{obs}(z/v) + \ln[NH_3]_0 \quad (1)$$

where k_{obs} is the pseudo-first-order loss rate constant, z is the injector position, v is the mean flow velocity, $[NH_3]_z$ is the gas-phase NH_3 concentration recorded by the QMS at position z,

and the subscript 0 is the initial reference position. Figure 1 shows a typical experimental result for NH_3 on an ice film at 190 K. The *x*-axis denotes the contact time, z/v, of NH_3 molecules on the ice surface; the time increases as the injector is pulled back to expose successively more ice surface. The *y*-axis represents the gas-phase NH_3 loss as detected by QMS. When NH_3 exposes to more ice surfaces, the loss of NH_3 on ice increases. The observed pseudo-first-order loss rate constant, k_{obs}, was determined from the least-squares fit of the experimental data ($t = 0-17.5$ ms) to eq 1. The injector was pushed back to the downstream end at $t \sim 40$ ms, as a check for the stability of the NH_3 signal (at $t > 40$ ms, the injector was at the fixed position). The plot shows that the NH_3 signal is stable, and there is no indication of adsorbed NH_3 to be desorbed from the ice surface. A value of $k_{obs} = 58.1\ s^{-1}$ at 189.7 K was obtained from the fit. k_{obs} was then corrected for gas-phase axial and radial diffusion by a standard procedure;[43] the corrected rate constant is termed k_w. The diffusion coefficient for NH_3 in helium was estimated to be 272.3 $cm^2 \cdot s^{-1}$ at 190 K and 1.0 torr.[44] The initial uptake coefficient γ_w was calculated from k_w using the following equation[45,46]

$$\gamma_w = 2Rk_w/(\omega + Rk_w) \quad (2)$$

where R is the radius of the flow reactor (0.85 cm) and ω is the mean NH_3 molecular velocity at the ice-film temperature.

It is generally accepted that the vapor-deposited ice film has internal surface areas and is porous. To obtain a "true" uptake coefficient γ_t, as if the film were a nonporous surface, γ_w is corrected for contributions due to the internal surfaces. On the basis of findings of previous studies, which were conducted under similar conditions,[47,48] ice films can be approximated as consisting of hexagonally close-packed spherical granules stacked in layers.[49] The true uptake coefficient, γ_t, is related to the value γ_w by

$$\gamma_t = \frac{\sqrt{3}\gamma_w}{\pi\{1 + \eta[2(N_L - 1) + (^3/_2)^{1/2}]\}} \quad (3)$$

where the effectiveness factor, $\eta = \phi^{-1} \tan h\phi$, is the fraction of the film surface that participates in the reaction, $\phi = ((N_L - 1)(^2/_3)^{1/2} + (^1/_2))[3\rho_b/2(\rho_t - \rho_b)](3\tau\gamma_t)^{1/2}$, where ρ_t and ρ_b are true density and bulk density of the ice, τ is tortuosity factor, and N_L is the number of granule layers.[49,50] Detailed calculations for these parameters can be found elsewhere.[47,49] A tortuosity factor $\tau = 4.4$, determined from fitting γ_w as a function of thickness (section 3.1.c), and a true ice density value $\rho_t = 0.925\ g \cdot cm^{-3}$ were used in the above calculation.

3. Results

3.1. Uptake of NH_3 on Ice Films. *3.1.a. Initial Uptake Coefficient of NH_3 on Ice Films.* In this set of experiments, the ice film was prepared by the water vapor deposition (section 2.2). Gaseous NH_3 was taken up by the ice-film surface as monitored by the QMS at $m/e = 16$; a typical result is shown in Figure 1. The initial uptake coefficient of NH_3 on ice films was studied as a function of partial NH_3 pressure at 189.8 ± 0.5 K. The results are presented in Figure 2, and detailed experimental conditions are listed in Table 1. Every k_{obs} or γ_w value in Table 1 was an average of two to five measurements, and every measurement was conducted on a freshly prepared ice film. The error bars in Figure 2 and the errors listed in Table 1 include both 1 standard deviation ± σ of the mean value and systematic errors related to the pressure gauges, digital thermometers, and mass flow meters, estimated collectively to be approximately 8%. Within the limited partial NH_3 pressure range (7.0×10^{-7} to 3.8×10^{-6} torr), the γ_w values fluctuate slightly, from 2.0×10^{-3} to 3.5×10^{-3}. Within the uncertainty of the measurement, the γ_w value is nearly independent of the partial pressure of NH_3 under our experiment conditions. The mean value of γ_w (shown as a solid line in Figure 2) is $(2.8 \pm 1.1) \times 10^{-3}$. The mean true uptake coefficient is $(3.8 \pm 1.4) \times 10^{-4}$ (Table 1). We did not study the initial uptake coefficient at warmer temperatures. At warmer temperatures (e.g., 230 K), the ice vapor pressure is higher, and the corresponding H_2O $m/e = 16$ fragment increases as well. This interference leads to a greater uncertainty in measuring the signal of NH_3 loss to ice surfaces.

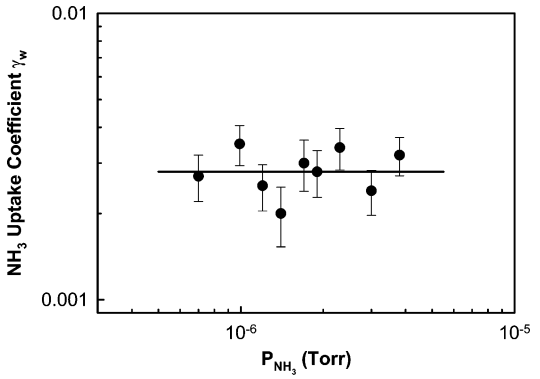

Figure 2. Plot of the initial uptake coefficient γ_w vs NH_3 partial pressure, for NH_3 uptake by the ice surface at 189.8 ± 0.5 K. The ice-film thickness was 3.5 ± 0.3 μm. The total pressure in the reactor was 0.500 ± 0.003 torr. The solid line shows the mean value of the experimental data points.

3.1.b. Effect of Ice-Film Thickness on Initial Uptake Coefficients. In this experiment, we varied the ice-film thickness, h, under a constant temperature. The initial uptake coefficient of NH_3 on the ice film increases quickly when the ice-film thickness $h < 10\ \mu$m; then, γ_w increases gradually as h increases at 190 K (shown in Figure 3). This behavior suggests that the ice film is porous and has internal surface areas. NH_3 molecules can gain access to internal surfaces by pore diffusion. We modeled this behavior using the hexagonally close-packed spherical granules pore-diffusion model.[49] Since N_L in eq 3 is a function of thickness, the solid line presented in Figure 3 is a result of a fitting of the data to eq 3. The relationship between N_L and h was assumed to be $N_L = a + b \log(h + c)$, where the parameters a, b, and c were determined from the nonlinear least-squares fit. The γ_t value was determined to be $(3.4 \pm 1.5) \times 10^{-4}$, and $\tau = 4.4 \pm 1.0$, from the nonlinear least-squares fit (see section 2.5). The detailed experimental conditions are also included in Figure 3.

3.1.c. Amount of NH_3 Uptake on Ice Film. A 20 cm length of ice film was prepared on the wall of the flow reactor at 189.2 K. Gas-phase NH_3 was admitted into the reactor via the movable injector. For the measurement of the amount of NH_3 uptake, the sliding injector was initially placed in the downstream end and in front of the ice film. A background signal was collected before NH_3 was admitted to the reactor. The initial NH_3 signal, as monitored by the QMS at $m/e = 16$, was recorded after NH_3 had been introduced into the reactor. Once the NH_3 signal had stabilized, the injector was quickly pulled out, toward the upstream end of the flow reactor, and the entire ice film was exposed to NH_3. The gas-phase NH_3 signal loss to the ice film was then recorded as a function of the exposure time. The amount of NH_3 uptake was determined by integration of the

TABLE 1: Uptake Coefficients of NH_3 on Ice Surfaces at 190 K[a]

temp (K)	P_{NH_3} (torr)	v (m/s)[b]	k_{obs} (1/s)	k_w (1/s)	γ_w	γ_t[c]
190.1 ± 0.6	7.0×10^{-7}	9.4	71.1 ± 9.1	80.7 ± 9.7	$(2.7 \pm 0.5) \times 10^{-3}$	$(3.6 \pm 0.7) \times 10^{-4}$
189.9 ± 0.3	9.9×10^{-7}	9.4	91.5 ± 10.5	99.2 ± 11.1	$(3.5 \pm 0.6) \times 10^{-3}$	$(4.8 \pm 0.9) \times 10^{-4}$
190.1 ± 0.4	1.2×10^{-6}	9.5	64.4 ± 8.2	72.4 ± 8.9	$(2.5 \pm 0.5) \times 10^{-3}$	$(3.4 \pm 0.7) \times 10^{-4}$
189.2 ± 0.6	1.4×10^{-6}	9.5	53.6 ± 7.0	58.7 ± 7.8	$(2.0 \pm 0.5) \times 10^{-3}$	$(2.7 \pm 0.7) \times 10^{-4}$
189.0 ± 0.2	1.7×10^{-6}	9.4	76.0 ± 10.3	87.3 ± 11.6	$(3.0 \pm 0.6) \times 10^{-3}$	$(4.1 \pm 0.8) \times 10^{-4}$
189.8 ± 0.5	1.9×10^{-6}	9.4	73.1 ± 8.8	82.3 ± 9.5	$(2.8 \pm 0.5) \times 10^{-3}$	$(3.8 \pm 0.7) \times 10^{-4}$
189.7 ± 0.4	2.3×10^{-6}	9.6	83.2 ± 12.2	96.3 ± 14.1	$(3.4 \pm 0.6) \times 10^{-3}$	$(4.6 \pm 0.9) \times 10^{-4}$
190.3 ± 0.4	3.0×10^{-6}	9.4	62.3 ± 7.6	68.9 ± 8.8	$(2.4 \pm 0.4) \times 10^{-3}$	$(3.2 \pm 0.6) \times 10^{-4}$
189.9 ± 0.7	3.8×10^{-6}	9.6	82.1 ± 9.7	95.5 ± 11.5	$(3.2 \pm 0.5) \times 10^{-3}$	$(4.3 \pm 0.7) \times 10^{-4}$
mean					$(2.8 \pm 1.1) \times 10^{-3}$	$(3.8 \pm 1.4) \times 10^{-4}$

[a] Total pressure was 0.500 ± 0.003 torr; ice-film thickness was 3.5 ± 0.3 μm at 189.8 ± 0.5 K. [b] Flow velocity. [c] γ_t was calculated from eq 3 by using $N_L = 2$, at 3.5 ± 0.3 μm.

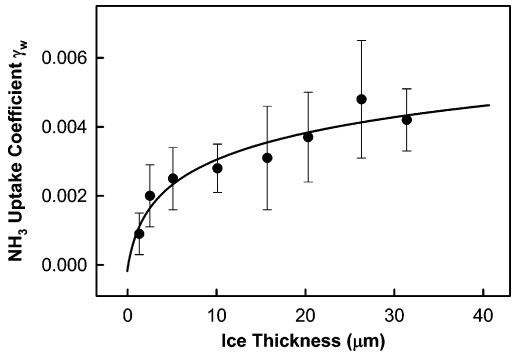

Figure 3. Plot of the initial uptake coefficient of NH_3, γ_w, on the ice as a function of the ice-film thickness, at 190 K. The total pressure in the reactor was 1.000 ± 0.003 torr, $P_{NH_3} = (2.0 \pm 0.3) \times 10^{-6}$ torr. The solid curve is a nonlinear least-squares fit to the data using eq 3 and an empirical correlation $N_L = a + b \log(h + c)$, where parameters a, b, and c were fitted to be $a = 0.22$, $b = 3.4$, and $c = 0.76$ (h = 1.3−31.4 μm). The plot shows that γ_w increases from 9.0×10^{-4} to 4.2×10^{-3} as the ice-film thickness increases. The γ_t value was determined to be $(3.4 \pm 1.5) \times 10^{-4}$.

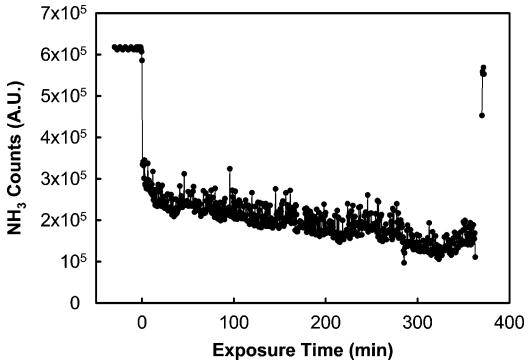

Figure 4. Plot of NH_3 signal vs exposure time, for NH_3 uptake by ice, at $P_{NH_3} = 1.4 \times 10^{-6}$ torr and 189.2 K. (●) represents the NH_3 signal. The plot shows the initial signal, before NH_3 came in contact with ice ($t < 0$), the uptake, starting at $t = 0$ min, when NH_3 was admitted onto the ice film, and the loss of NH_3 on the ice film. The injector was pushed back to the downstream end (line break) as a check of the stability of the NH_3 signal. No measurable NH_3 desorption from the ice surface was found. The NH_3 background signal was subtracted. The amount of NH_3 taken up by ice was $>2.9 \times 10^{15}$ molecules/cm^2, based on the total ice surface area. The total pressure was 1.0 torr, and ice-film thickness was 3.2 μm.

calibrated NH_3 signal over the exposure time. This is shown in Figure 4. The amount of NH_3 uptake was determined to be $>2.2 \times 10^{16}$ molecules/cm^2 on ice film at 189.2 K, as calculated from the geometric surface area of the reactor (Figure 4), after the ice film had been exposed to NH_3 for ~7 h; that length of time was too short to permit steady-state equilibrium to be reached. Even after we take the porosity of the ice film into consideration, the amount of NH_3 uptake is estimated to be $>2.9 \times 10^{15}$ molecules/cm^2 on the basis of the total ice surface area, which was estimated using the ratio of the total ice surface area to the geometric area $= 3^{-1/2}\pi[2N_L - 1 + (3/2)^{1/2}]$.[49] This high amount of NH_3 taken up by the ice surface is likely due to the formation of metastable hydrates or peritectic liquid.[51−54] NH_3 is known to form hydrates at low temperatures,[18,22,51−54] as will be discussed in the Discussion section. However, the details are beyond the scope of this work and will be the subject of future studies.

The stability of the m/e =16 signal is a concern in this experiment, because of the long time duration. At the end of the measurement, the injector was pushed back to the downstream end position, and the NH_3 signal was measured at $t \geq$ 370 min, as a check of the stability of the NH_3 signal. The NH_3 signal at the end is approximately the same as the initial signal ($t < 0$ min), within the uncertainty of the measurement. The $m/e = 16$ signal fluctuation in Figure 4 derives from both the variation of the ice vapor pressure due to small temperature fluctuations (±0.3 K) in the flow reactor and the pressure changes of the QMS vacuum system over ~7 h. A small drift in $m/e = 16$ baseline is mainly due to evacuation of water vapor in the QMS vacuum system over the experimental time period. This factor was taken into consideration when we calculated the amount of NH_3 uptake. Note that the magnitude of the $m/e = 16$ signal drift over 6−7 h is comparable with the signal random fluctuation depicted in Figure 4. An average background $m/e = 16$ signal determined before the uptake measurement was subtracted from the data before plotting. Both Figures 1 and 4 also suggest that NH_3 taken up by the ice should not be desorbed from the ice surface within the experimental time frames. Additional experiments (data not shown) confirmed that adsorbed NH_3 does not desorb from the ice surface as the injector is pushed back to the downstream end; we thus conclude that adsorption of NH_3 on ice is irreversible.

3.2. Reaction Probability of NH_3 on HOBr−Ice Films. Once the ice film was deposited on the wall of the flow reactor, freshly prepared ice was exposed to HOBr, as the sliding injector was slowly pulled out toward the upstream end, to uncover the entire ice-film surface. The surface coverage of HOBr, taken up by the ice film, was determined by integration of the HOBr signal (m/e = 96) over the exposure time. The result was expressed as the amount of HOBr taken by both the geometric surface area and the total ice surface area (Table 2). We varied either the HOBr flow rate (5−30 sccm) or partial HOBr pressure (typical $P_{HOBr} = 1.6 \times 10^{-6}$ torr), or a combination of the two, to achieve a range of HOBr surface coverages. The saturation

TABLE 2: Reaction Probability of NH_3 on HOBr-Treated Ice Surfaces[a]

temp K	P_{NH_3} (torr)	v (m/s)	HOBr surface coverage (molecules/cm^2)[b]	corrected surface coverage[c]	k_{obs} (1/s)	k_w (1/s)	γ_w	γ_t[d]
190.0 ± 0.3	1.4×10^{-6}	8.4	$(1.6 \pm 0.2) \times 10^{14}$	2.1×10^{13}	81.6 ± 11	89.0 ± 12	$(3.1 \pm 0.5) \times 10^{-3}$	$(4.2 \pm 0.7) \times 10^{-4}$
190.2 ± 0.4	1.3×10^{-6}	8.5	$(3.1 \pm 0.2) \times 10^{14}$	4.1×10^{13}	116 ± 21	131 ± 24	$(4.5 \pm 1.0) \times 10^{-3}$	$(6.2 \pm 1.5) \times 10^{-4}$
190.0 ± 0.3	1.3×10^{-6}	8.5	$(6.1 \pm 0.2) \times 10^{14}$	8.0×10^{13}	87.9 ± 17	96.5 ± 20	$(3.4 \pm 0.7) \times 10^{-3}$	$(4.6 \pm 1.0) \times 10^{-4}$
190.0 ± 0.3	1.4×10^{-6}	8.4	$(7.9 \pm 0.3) \times 10^{14}$	1.0×10^{14}	125 ± 24	143 ± 29	$(5.0 \pm 1.0) \times 10^{-3}$	$(6.9 \pm 1.5) \times 10^{-4}$
189.8 ± 0.5	1.4×10^{-6}	8.4	$(1.1 \pm 0.1) \times 10^{15}$	1.4×10^{14}	109 ± 18	123 ± 22	$(3.7 \pm 1.2) \times 10^{-3}$	$(5.1 \pm 1.7) \times 10^{-4}$
190.2 ± 0.4	1.4×10^{-6}	8.2	$(1.6 \pm 0.2) \times 10^{15}$	2.1×10^{14}	88.9 ± 13	98.1 ± 15	$(3.5 \pm 0.6) \times 10^{-3}$	$(4.8 \pm 0.9) \times 10^{-4}$

[a] Total pressure was 0.500 ± 0.003 torr; HOBr-treated ice-film thickness was 3.4 ± 0.2 μm at 190.0 ± 0.4 K. [b] HOBr surface coverage based on the geometric surface area. [c] HOBr coverage (molecules/cm^2) over the total ice surface area, which was calculated using the ratio of the total ice surface to the geometric surface area in the cylindrical flow reactor = $3^{-1/2}\pi[2N_L - 1 + (3/2)^{1/2}]$ and $N_L = 2$. [d] γ_t was calculated from eq 3 by using $N_L = 2$, at 3.4 ± 0.2 μm.

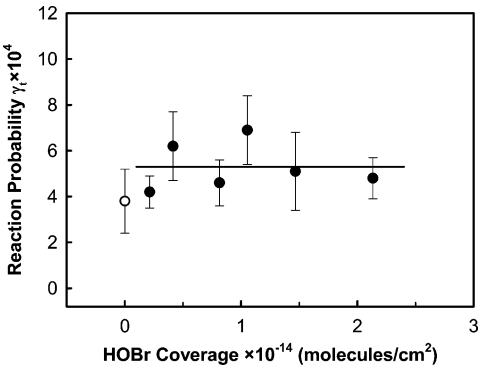

Figure 5. Plot of the reaction probability γ_t of NH_3 on HOBr-treated ice surfaces (●) vs HOBr surface coverage (total ice surface area), at 190 K. The thickness of the ice film was 3.4 ± 0.2 μm. The partial pressure of NH_3 was $(1.3 \pm 0.2) \times 10^{-6}$ torr, and the total pressure in the reactor was 0.500 ± 0.003 torr. The solid line represents the mean value of the data points. The true uptake coefficient of NH_3 on the ice surface (○) is included in the plot.

HOBr coverage was determined to be $(2.7 \pm 0.6) \times 10^{14}$ molecules/cm^2 (total surface area) at $P_{HOBr} = 1.6 \times 10^{-6}$ torr and 190 K. After the ice film had been treated with HOBr, the injector was pushed back to the downstream end. It is important to point out that adsorbed HOBr remains on the ice surface (i.e., there is no measurable HOBr desorption) when the injector is pushed back to the downstream end. This was demonstrated in our previous studies as well.[42,46] Gas-phase NH_3 at a pressure of $(1.3 \pm 0.2) \times 10^{-6}$ torr was admitted to the system, and the HOBr-treated ice-film surface was then exposed. The injector was pulled out toward the upstream end, in 2 cm increments. The loss of NH_3 was measured by the QMS as a function of the injector distance z. The pseudo-first-order rate constant, k_{obs}, and the reaction probability, γ_w, for NH_3 on the HOBr-treated ice film were determined using eqs 1 and 2, respectively. The amount of NH_3 taken up by the HOBr-treated ice surface during the entire measurement was $< 1 \times 10^{13}$ molecules/cm^2, and the pseudo-first-order rate treatment is valid. We measured γ_w as a function of the HOBr surface coverage (molecules/cm^2) at 190.0 ± 0.4 K. The true reaction probability, γ_t, was calculated from the γ_w value, by use of eq 3. The results are shown in Figure 5, and detailed experimental conditions are presented in Table 2. The values reported in Table 2 were an average of two to three measurements. The errors listed in Table 2 and the error bars in Figure 5 include both 1 standard deviation ± σ of the mean value and systematic errors. Figure 5 shows that the γ_t value does not significantly change as the HOBr surface coverage increases from 2.1×10^{13} to 2.1×10^{14} molecules/cm^2, as calculated based on the total ice surface area, at 190 K; the value remains approximately $(5.3 \pm 2.2) \times 10^{-4}$. This value is slightly higher than γ_t of NH_3 on ice at 190 K.

4. Discussion

4.1. Uptake of NH_3 by Ice Films. *4.1.a. Uptake of NH_3 by Ice*. Figure 4 shows that the amount of NH_3 taken up by ice ($> 2.9 \times 10^{15}$ molecules/cm^2) exceeds monolayer surface coverage. Using the van der Waals radius of N and H,[55] we estimated the size of the NH_3 molecule on a surface to be ~40 Å.[2] The corresponding monolayer surface coverage is approximately 2.4×10^{14} NH_3 molecules/cm^2. A possible explanation for multilayer adsorption is as follows: When NH_3 is adsorbed to the ice surface, NH_3 is expected to be bound by H_2O or hydrated on the ice surface due to strong hydrogen bonding between NH_3 and H_2O, as has been demonstrated experimentally.[20,26] Once NH_3 accumulates near the surface, we anticipate the formation of NH_3 (metastable) hydrates or peritectic liquids at 190 K.[54] Pursell et al. showed the formation of $NH_3(H_2O)_n$ at $T > 140$ K.[18]

The thermodynamic phases of NH_3 in ice are hydrates or peritectic liquid at 190 K, depending on the equilibrium NH_3 pressure or NH_3−ice composition, according to the NH_3−ice phase diagram.[54] Although gas−surface equilibrium is not reached in the experiment depicted in Figure 4, either metastable hydrates or peritectic liquid would explain the experimental data in the figure, because the topmost bilayers of the ice surface would require stoichiometrically equivalent layers of NH_3 to form an NH_3−H_2O complex. Additional supporting evidence is that the observed uptake profile in Figure 4 resembles the profiles for either HBr or HNO_3 hydrates near the ice surface at 188 K.[38,50,56]

We rule out the possibility that behavior depicted in Figure 4 is due to the diffusion of NH_3 into bulk ice. Assuming that the diffusion coefficient D of NH_3 in ice is similar to that of H_2O in ice (~10^{-11} to 10^{-12} cm^2/s[57]) at 190 K (since the two D values are similar at 110 K[22,58]), the time required for NH_3 to diffuse over $x = 3.2$ μm ice is estimated to be ~3 h, according to $t \approx x^2/2D$. There is no indication of NH_3 signal recovery even at >6 h (Figure 4), suggesting that some process other than diffusion is the determinant.

The rapid loss of the NH_3 signal on ice at $t = 0$ (Figure 4) also reflects the loss rate or uptake coefficient of NH_3 on ice. The difference between the initial uptake coefficient measured based on the plot in Figure 1 and the loss rate taken from the plot at $t = 0$ in Figure 4 is as follows: A fresh ice surface was exposed to NH_3 one section at a time with well-controlled gas−surface contact time, approximately milliseconds, in the experiment shown in Figure 1. In the experiment shown in Figure 4, the injector was pulled out to expose the entire ice surface to NH_3 and the real time was recorded. This is equivalent to the NH_3 loss of two data points in Figure 1, one taken at $t = 0$ and the other taken just before the injector is pushed back, with less precisely controlled gas−surface contact time and with less cleanness of the ice surface (uptake coefficient is a function of

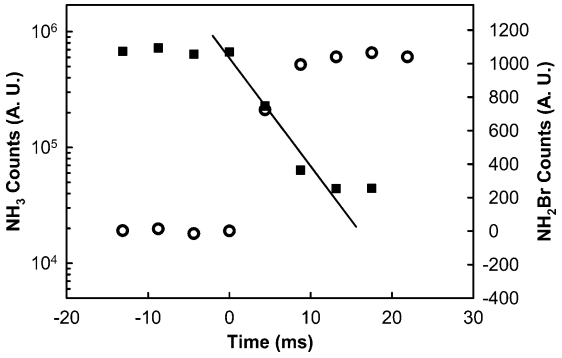

Figure 6. Possible products of the heterogeneous reaction of NH_3 + HOBr on the ice surface at 190 K. (■) represents the NH_3 signal, and (○) represents the NH_2Br signal. A plot of the NH_3 signal loss vs the time is shown on the left-hand *y*-axis. The formation of NH_2Br, detected by QMS at $m/e = 94$, is shown on the right-hand *y*-axis of the plot. The combination of the plots suggests that bromination of NH_3 is occurring between HOBr and NH_3, with NH_2Br as the product. See text for details.

surface coverage[36]). Thus, we did not determine the uptake coefficient from the data in Figure 4.

4.1.b. Uptake Coefficient of NH_3 on Ice. The experimental results indicated that the initial uptake coefficient of NH_3 on the ice surface at 190 K is approximately 2.8×10^{-3} (Figure 2), and the data in Figure 4 suggest that no obvious surface saturation effect occurs on a time scale of minutes. The γ values in Figure 2 are expected according to the precursor model,[36] which is illustrated in the equations

$$NH_3(g) \underset{k_{-1}}{\overset{k_1}{\rightleftharpoons}} NH_3\ (\text{precursor}) \xrightarrow{k_2} NH_3(ad) \tag{4}$$

The loss rate of NH_3 is given by

$$-\frac{d[NH_3(g)]}{dt} = k_1[NH_3(g)] - k_{-1}[NH_3(p)] \tag{5}$$

The precursor $[NH_3(p)]$ can be determined using the steady-state approximation $d[NH_3(p)]/dt = 0$, and eq 5 can be rewritten as

$$-\frac{d[NH_3(g)]}{dt} = \frac{k_1k_2}{k_{-1} + k_2}[NH_3(g)] \tag{6}$$

The uptake coefficient can be expressed as

$$\gamma = \frac{-\dfrac{d[NH_3(g)]}{dt}}{\dfrac{[NH_3(g)]\omega}{4}\dfrac{S}{V}} = \frac{4k_1k_2}{\omega(k_{-1} + k_2)}\frac{V}{S} \tag{7}$$

where ω is the mean molecular velocity of NH_3 and S/V is the surface-to-volume ratio of the flow reactor. Equation 7 indicates that the uptake coefficient for NH_3 on the ice surface at constant temperature is independent of the partial pressure of NH_3. This is in agreement with the experimental data plotted in Figure 2.

4.2. NH_3 Reaction with HOBr-Treated Ice Films. The reaction probability, γ_t, was determined as a function of the HOBr surface coverage (molecules/cm^2) at 190 K. In this experiment, the ice surface was treated with HOBr molecules first, and HOBr coverage was determined. Figure 5 shows that the measured γ_t value is nearly independent of HOBr coverage. A product, NH_2Br, was detected in the gas phase (Figure 6). We have determined that the mean γ_t for NH_3 on ice surfaces is 3.8×10^{-4} at 190 K (Table 1). On the basis of our previous work and the findings of this study, we concluded that HOBr molecules are adsorbed on ice surfaces at 190 K with $\gamma_w \approx 0.1$.[42] These evidences suggest that both HOBr and NH_3 molecules can be adsorbed to the ice surface, and the reaction then proceeds. However, the observed reaction probability is equal to or slightly higher than γ_t of NH_3 on ice (see Figure 5). This leads us to propose that the reaction occurs when NH_3 migrates and collides with HOBr already adsorbed on the surface. This sequence of events is described as

$$HOBr(g) + S_1 \underset{k_{-3}}{\overset{k_3}{\rightleftharpoons}} HOBr(ad) \tag{8}$$

$$NH_3(g) + S_2 \underset{k_{-4}}{\overset{k_4}{\rightleftharpoons}} NH_3(ad) \tag{9}$$

$$HOBr(ad) + NH_3(ad) \xrightarrow{k_5} NH_2Br(g) + H_2O(ad) + S_2 \tag{10}$$

We assume that HOBr and NH_3 are independently adsorbed on different ice surface sites S_1 and S_2. HOBr surface coverage is on the order of a submonolayer. Our experimental condition was that the amount of NH_3 taken up by ice is lower than the amount of HOBr surface coverage. NH_3 has a higher probability of finding an ice surface site than an HOBr−ice site, at low θ_{HOBr}. This approximation becomes invalid as $\theta_{HOBr} > 0.5$, where θ_{HOBr} is the HOBr surface coverage. Although it is also possible that NH_3 adsorbs on top of HOBr(ad), we will not distinguish these situations. Reaction 10 is based on the fact that NH_2Br was detected by the QMS in the gas phase. We expect that the rate for reaction 10 is greater than or equal to the rate for reaction 9, because the reaction probability is slightly greater than γ_t of NH_3 on ice (Figure 5). An expression for the reaction probability can be derived using the approach described as follows. The rate of the reaction can be expressed by the observed loss rate of NH_3:

$$-\frac{d[NH_3(g)]}{dt} = k_4[NH_3(g)][S_2] - k_{-4}\theta_{NH_3} \tag{11}$$

where θ_{NH_3}, the NH_3 surface coverage, can be determined using the steady-state approximation, $d[\theta_{NH_3}]/dt = 0$. Equation 11 can be rewritten as

$$-\frac{d[NH_3(g)]}{dt} = \frac{k_4k_5\theta_{HOBr}}{k_{-4} + k_5\theta_{HOBr}}[NH_3(g)][S_2] \tag{12}$$

where θ_{HOBr} is the HOBr surface coverage. The reaction probability, γ_t, can be expressed as

$$\gamma_t = \frac{-\dfrac{d[NH_3(g)]}{dt}}{\dfrac{[NH_3(g)]\omega}{4}\dfrac{S}{V}} = \frac{4k_4k_5V\theta_{HOBr}}{\omega S(k_{-4} + k_5\theta_{HOBr})}[S_2] \tag{13}$$

where ω is the mean molecular velocity of NH_3. In our experiment, we chose $\theta_{HOBr} > \theta_{NH_3}$ so as to satisfy the pseudo-first-order approximation for the experimental measurement. For moderate HOBr coverage, we anticipate that $k_5\theta_{HOBr} > k_{-4}$, because the reaction probability is greater than or equal to γ_t of NH_3 on ice (Figure 5). Equation 13 can be simplified to

$$\gamma_t = \frac{4k_4}{\omega}\frac{V}{S}[S_2] \tag{14}$$

Since the initial S_2 site, $[S_2^o] = [S_2] + NH_3(ad)$, $[S_2] = S_2^o/(1 + k_4[NH_3(g)]/k_{-4})$, eq 14 can be written as

$$\gamma_t = \frac{4k_4}{\omega}\frac{V}{S}\frac{S_2^o}{1 + k_4[NH_3(g)]/k_{-4}} \quad (15)$$

We employed a fixed value for P_{NH_3}, and θ_{NH_3} ($\leq 10^{13}$ molecules/cm^2) is nearly constant. As a first-order approximation, $[S_2]$ is roughly constant. Equation 15 suggests that γ_t is independent of HOBr surface concentration at 190 K; that is in agreement with the result shown in Figure 5. The solid line in the figure depicts the mean value of $\gamma_t = (5.3 \pm 2.2) \times 10^{-4}$ of the experimental data points.

The above analysis suggests that, for the heterogeneous reaction that occurs between HOBr and NH_3 on the ice surface at 190 K, the reaction probability is a function of $[NH_3]$ and depends on available surface sites for NH_3 adsorption (reaction 9 and eq 14). If reaction 10 correctly depicts the product for the reaction, we should be able to detect the gas-phase product NH_2Br. Figure 6 shows both the formation of NH_2Br and the loss of NH_3 experimentally. The NH_3 signal is plotted on the left-hand *y*-axis, and the NH_2Br signal is on the right-hand *y*-axis. The NH_3 signal tailing off at a late time (~20 ms) was likely due to some ice surface sites having been adsorbed by NH_3, and thus the uptake rate was modified. This behavior was also observed in Figure 1. These tailing off points were not included in the γ_w calculation because we intended to determine the initial uptake coefficient. The plot shows that the NH_3 signal decreases as the reaction proceeds, and the product NH_2Br, detected by the QMS at $m/e = 94$, is increasingly desorbed from the surface. The data in Figure 6 thus support our proposed reaction pathway. Analogous to the reaction in solution,[30] we expect that NH_2Br will further react with adsorbed HOBr, to produce $NHBr_2$. A disproportion reaction for NH_2Br can occur under weakly basic conditions.[31] Due to both the low signal intensity for NH_2Br production and side reactions, we cannot obtain reliable rate constants from the formation of NH_2Br.

4.3. Comparison with Results of Previous Studies. We can compare our results with the findings from other relevant studies of NH_3 interaction at water interfaces and on *n*-hexane soot surfaces. Muenter and Koehler employed the transmission FTIR technique to quantify NH_3 taken up by *n*-hexane soot surfaces between 115 and 153 K, with $P_{NH_3} \sim 10^{-3}$ torr.[13] The values for the uptake coefficient determined in that study ranged from $\sim 0.02 \pm 0.01$ at 115 K to $\geq (1.5 \pm 0.8) \times 10^{-4}$ at 153 K. We have in the present study determined the initial uptake coefficient γ_w to be 2.8×10^{-3} for NH_3 on ice-film surfaces at 190 K, and with P_{NH_3} in the range of 7.0×10^{-7} to 3.8×10^{-6} torr. It is predicted that NH_3 has a higher uptake coefficient on ice, because of hydrogen-bonding interactions.[4,20,26] An indicator of this is that the uptake coefficient of NH_3 at the water surface is 0.1−0.3 at 290−260 K.[16,17,25] Donaldson reported the saturated coverage of ammonia to be $(1.2 \pm 0.2) \times 10^{14}$ molecules/cm^2 at a water interface at 298 K.[15] We have determined that the lower limit of the amount of NH_3 taken up by ice is $>2.9 \times 10^{15}$ molecules/cm^2 at 190 K. The higher uptake amount at the ice surface reflects the possible formation of metastable hydrates or peritectic liquid near the ice surface.[51−54]

There are no previously published results on the reaction probability of NH_3 on HOBr-treated ice surfaces. The reaction between NH_3 and HOBr in aqueous solution has been studied, and the rate constants for the reactions

$$HOBr + NH_3 \xrightarrow{k_6} NH_2Br + H_2O \quad (16)$$

$$BrO^- + NH_3 \xrightarrow{k_7} NH_2Br + OH^- \quad (17)$$

were, respectively, found to be $k_6 = 7.5 \times 10^7$ M^{-1} s^{-1} and $k_7 = 7.6 \times 10^4$ M^{-1} s^{-1} at 293 K.[31] Because these specific rate constants were determined in solution, we cannot make a direct comparison between the reported aqueous values and the γ values obtained from our present study. The reaction rates are affected by the pH of the solution. We assume that the reaction probability of NH_3 on HOBr-treated ice surfaces is also affected by the pH at ice surfaces. The pK_a value of HOBr is ~8.8 at 298 K.[59] This implies that $[HOBr] > [OBr^-]$ in a neutral or slightly acidic environment. For example, at pH = 7, $[HOBr]/[OBr^-] = 120$. If we accept that the reaction between HOBr and NH_3 on ice is analogous to the reaction in solution, then the rate of reaction 16 is faster than that of reaction 17.

4.4. Atmospheric Implications. NH_3 plays an important role in neutralizing acidic atmospheric aerosols. The reactive uptake coefficient for NH_3 on sulfuric acid solutions is ~1.[25,60] We have determined that the reaction probability, γ_t, of NH_3 on HOBr−ice is 5.3×10^{-4} at 190 K; the γ_t value is expected to be lower at warmer temperatures. To illustrate the relative importance of two loss processes in the Arctic boundary layer, we estimate NH_3 heterogeneous atmospheric lifetimes due to the NH_3 + HOBr reaction on ground-level snow-ice surfaces and the loss on Arctic haze sulfate aerosols. The NH_3 heterogeneous atmospheric lifetime τ on haze sulfate aerosols can be calculated from

$$\tau = 4/\gamma\omega A_c \quad (18)$$

where A_c is an aerosol surface to air volume ratio. Using typical $A_c \approx 10^{-4}$ cm^2/cm^3 and $\gamma = 0.5-1$,[60,61] $\tau \approx 1-2$ s at 250 K. The calculation of the NH_3 lifetime on a surface of snow-ice involves transporting NH_3 in the boundary layer and NH_3 heterogeneous loss on HOBr−ice surfaces. Here, we will estimate the heterogeneous reaction lifetime of NH_3 on HOBr−ice/snow surfaces. The specific surface area of Arctic fresh snow is approximately 500 cm^2/g and the density ≈0.4 g/cm^3.[62,63] Assuming the reaction between NH_3 and HOBr occurs near the surface of the snow-ice layer (~50−100 μm), because pore diffusion of NH_3 into inner snow layers is limited as suggested by Figure 3, using $\gamma \approx 10^{-5}$ (HOBr coverage ~10^{13} molecules/cm^2) and $A_c \approx 1$ cm^2/cm^3 at 250 K,[64] heterogeneous atmospheric lifetime for NH_3 on HOBr−ice is estimated to be $\tau \approx 10$ s. The heterogeneous atmospheric NH_3 loss rate by HOBr−ice is slower than that by haze sulfate aerosols ($\gamma \sim 1$). A fraction of the NH_3 molecules is neutralized by haze sulfate aerosols when NH_3 is transported from the atmospheric surface layer (~100 m) to ground-level snow surfaces because the dry deposition velocity is slow, ~1 cm/s.[6] In addition, the heterogeneous reaction between HOBr and HCl on ice surfaces has a reaction probability $\gamma_t > 0.01$ at 189.5 K and HOBr coverage ~10^{13} molecules/cm^2.[42] Thus, the NH_3 heterogeneous removal rate due to the reaction between NH_3 and HOBr on ground-level ice/snow is not as significant as the rate of NH_3 neutralization by sulfuric acid aerosols in the Arctic boundary layer.

5. Summary

We have studied the uptake of NH_3 on ice surfaces, and the reaction of NH_3 with HOBr-treated ice surfaces, using a low-temperature flow reactor coupled with a differentially pumped

QMS. The true uptake coefficient γ_t of NH_3 has been determined to be $(3.8 \pm 1.4) \times 10^{-4}$ on ice films at 189.8 K, for a NH_3 partial pressure ranging from 7.0×10^{-7} to 3.8×10^{-6} torr. The lower limit of the amount of NH_3 uptake is $>2.9 \times 10^{15}$ molecules/cm^2 on the ice-film surface at 189.2 ± 0.5 K. The reaction probability γ_t of NH_3 + HOBr was determined to be $\sim(5.3 \pm 2.2) \times 10^{-4}$, over a range of HOBr surface coverages from 2.1×10^{13} to 2.1×10^{14} molecules/cm^2, at 190.0 ± 0.4 K. The reaction probability is nearly independent of the HOBr surface coverage. Comparison with the rate of NH_3 neutralization on sulfuric acid aerosols in the boundary layer suggests that atmospheric removal rate of NH_3 by HOBr on snow-ice surfaces is not a major pathway at typical boundary-layer temperatures; at such temperature, γ of NH_3 + HOBr is expected to be yet lower than the value that we have determined at 190 K.

Acknowledgment. The authors thank Ms. Hui Yan for her assistance during the course of this study and Dr. Leon Keyser for helpful discussion. This work was supported by the National Science Foundation under Grant ATM-0355521.

References and Notes

(1) Abbatt, J. P. D. *Chem. Rev.* **2003**, *103*, 4783.
(2) Gertner, B. J.; Hynes, J. T. *Science* **1996**, *271*, 1563.
(3) Kang, H.; Shin, T.-H.; Park, S.-C.; Kin, I. K.; Ham, S.-J. *J. Am. Chem. Soc.* **2000**, *122*, 9842.
(4) Girardet, C.; Toubin, C. *Surf. Sci. Rep.* **2001**, *44*, 159.
(5) Levine, J. S.; Augustsson, T. R.; Hoell, J. M. *Geophys. Res. Lett.* **1980**, *7*, 317.
(6) Finlayson-Pitts, B. J.; Pitts, J. N., Jr. *Chemistry of the Upper and Lower Atmosphere*; Academic Press: San Diego, CA, 2000.
(7) Jacob, D. J.; Hoffmann, M. R. *J. Geophys. Res.* **1983**, *88*, 6611.
(8) Myles, L; Meyers, T. P.; Robinson, L. *Atmos. Environ.* **2006**, *40*, 5745.
(9) Kerminen, V. M.; Wexler, A. S.; Potukuchi, S. *J. Geophys. Res.* **1997**, *102*, 3715.
(10) Weber, R. J.; Marti, J. J.; McMurry, P. H.; Eisele, F. L.; Tanner, D. J.; Jefferson, A. *Chem. Eng. Commun.* **1996**, *151*, 53.
(11) Coffman, D. J.; Hegg, D. A. *J. Geophys. Res.* **1995**, *100*, 7147.
(12) Abbatt, J. P. D.; Benz, S.; Cziczo, D. J.; Kanji, Z.; Lohmann, U.; Möhler, O. *Science* **2006**, *313*, 1770.
(13) Muenter, A. H.; Koehler, B. G. *J. Phys. Chem. A* **2000**, *104*, 8527.
(14) Duncan, L. C. *Environ. Sci. Technol.* **1992**, *26*, 61.
(15) Donaldson, D. J. *J. Phys. Chem. A* **1999**, *103*, 62.
(16) Shi, Q.; Davidovits, P.; Jayne, J. T.; Worsnop, D. R.; Kolb, C. E. *J. Phys. Chem. A* **1999**, *103*, 8812.
(17) Ponche, J. L.; George, C.; Mirabel, P. *J. Atmos. Chem.* **1993**, *16*, 1.
(18) Pursell, C. J.; Zaidi, M.; Thompson, A.; Fraser-Gaston, C.; Vela, E. *J. Phys. Chem. A* **2000**, *104*, 552.
(19) Souda, R. *J. Chem. Phys.* **2003**, *119*, 2774.
(20) Ogasawara, H.; Horimot, N.; Kawai, M. *J. Chem. Phys.* **2000**, *112*, 8229.
(21) Delzeit, L.; Powell, K.; Uras, N.; Devlin, J. P. *J. Phys. Chem. B* **1997**, *101*, 2327.
(22) Uras, N.; Devlin, J. P. *J. Phys. Chem. A* **2000**, *104*, 5770.
(23) Uras, N.; Buch, V.; Devlin, J. P. *J. Phys. Chem. B* **2000**, *104*, 9203.
(24) Bertie, J. E.; Devlin, J. P. *J. Chem. Phys.* **1984**, *81*, 1559.
(25) Davidovits, P.; Kolb, C. E.; Williams, L. R.; Jayne, J. T.; Worsnop, D. R. *Chem. Rev.* **2006**, *106*, 1323.
(26) Kondo, M.; Kawanowa, H.; Gotoh, Y.; Souda, R. *Surf. Sci.* **2005**, *594*, 141.
(27) Pinkernell, U.; von Gunten, U. *Environ. Sci. Technol.* **2001**, *35*, 2525.
(28) Armesto, X. L.; Canle, L. M.; Santaballa, J. A. *Chem. Soc. Rev.* **1998**, *27*, 453.
(29) Bousher, A.; Brimblecombe, P.; Midgley, D. *Water Res.* **1989**, *23*, 1049.
(30) Galal-Gorchev, H.; Morris, J. C. *Inorg. Chem.* **1965**, *4*, 899.
(31) Wajon, J. E.; Morris, J. C. *Inorg. Chem.* **1982**, *21*, 4258. The observed second-order rate constant is a function of acidity. $k = 2.6 \times 10^5$ M^{-1} s^{-1} at pH = 7, ionic strength = 0.013 M, and 20 °C for the HOBr + NH_3 reaction.
(32) Inman, G. W.; Johnson, J. D. *Environ. Sci. Technol.* **1984**, *18*, 219.
(33) Lei, H.; Marinas, B. J.; Minear, R. A. *Environ. Sci. Technol.* **2004**, *38*, 2111.
(34) Norman, M.; Leck, C. *J. Geophys. Res.* **2005**, *110*, D16302.
(35) Impey, G. A.; Mihele, C. M.; Anlauf, K. G.; Barrie, L. A.; Shepson, P. B. *J. Atmos. Chem.* **1999**, *34*, 21.
(36) Masel, R. I. *Principles of Adsorption and Reaction on Solid Surfaces*; Wiley: New York, 1996.
(37) Chu, L.; Chu, L. T. *J. Phys. Chem. A* **1999**, *103*, 691.
(38) Chu, L. T.; Heron, J. W. *Geophys. Res. Lett.* **1995**, *22*, 3211.
(39) Chu, L. T. *J. Vac. Sci. Technol., A* **1997**, *15*, 201.
(40) Keyser, L. F.; Leu, M.-T. *J. Colloid Interface Sci.* **1993**, *155*, 137.
(41) Jin, R. H.; Chu, L. T. *J. Phys. Chem. A* **2006**, *110*, 3647.
(42) Chu, L.; Chu, L. T. *J. Phys. Chem. A* **1999**, *103*, 8640.
(43) Brown, R. L. *J. Res. Natl. Bur. Stand. (U.S.)* **1978**, *83*, 1.
(44) Cussler, E. L. *Diffusion, Mass Transfer in Fluid Systems*; Cambridge University Press: New York, 1984; Chapter 4.
(45) Chu, L. T.; Leu, M.-T.; Keyser, L. F. *J. Phys. Chem.* **1993**, *97*, 12798.
(46) Jin, R.; Chu, L. T. *J. Phys. Chem. A* **2006**, *110*, 8719.
(47) Keyser, L. F.; Moore, S. B.; Leu, M.-T. *J. Phys. Chem.* **1991**, *95*, 5496.
(48) Keyser, L. F.; Leu, M.-T. *Microsc. Res. Tech.* **1993**, *25*, 343.
(49) Keyser, L. F.; Leu, M.-T.; Moore, S. B. *J. Phys. Chem.* **1993**, *97*, 2800.
(50) Chu, L. T.; Leu, M.-T.; Keyser, L. F. *J. Phys. Chem.* **1993**, *97*, 7779.
(51) Fortes, A. D.; Brodholt, J. P.; Wood, I. G.; Vočadlo, L.; Jenkins, H. D. B. *J. Chem. Phys.* **2001**, *115*, 7006.
(52) Fortes, A. D.; Wood, I. G.; Brodholt, J. P.; Alfredsson, M.; Vočadlo, L.; McGrady, G. S.; Knight, K. S. *J. Chem. Phys.* **2003**, *119*, 10806.
(53) Fortes, A. D.; Wood, I. G.; Brodholt, J. P.; Vočadlo, L. *Icarus* **2003**, *162*, 59.
(54) Kargel, J. S. *Icarus* **1992**, *100*, 556.
(55) Bondi, A. *J. Phys. Chem.* **1964**, *68*, 441.
(56) Chu, L. T.; Chu, L. *J. Phys. Chem. A* **1999**, *103*, 384.
(57) Brown, D. E.; George, S. M. *J. Phys. Chem.* **1996**, *100*, 15460.
(58) Jung, K.-H.; Park, S.-C.; Kim, J.-H.; Kang, H. *J. Chem. Phys.* **2004**, *121*, 2758.
(59) Troy, R. C.; Margerum, D. W. *Inorg. Chem.* **1991**, *30*, 3538.
(60) *Chemical Kinetics and Photochemical Data for Use in Atmospheric Studies—Evaluation Number 15*; JPL Publication 06-2; NASA JPL: Pasadena, CA, 2006.
(61) Kolb, C. E.; Worsnop, D. R.; Zahniser, M. S.; Davidovits, P.; Keyser, L. F.; Leu, M.-T.; Molina, M. J.; Hanson, D. R.; Ravishankara, A. R.; Williams, L. R.; Tolbert, M. A. In *Progress and Problems in Atmospheric Chemistry*; Baker, J. R., Ed.; World Scientific: Singapore, 1995; Chapter 18.
(62) Cabanes, A.; Legagneux, L.; Dominé, F. *Atmos. Environ.* **2002**, *36*, 2767.
(63) Dominé, F.; Cabanes, A.; Legagneus, L. *Atmos. Environ.* **2002**, *36*, 2753.
(64) Choose 1 cm^3 air volume, and the reaction occurs on the top 50 μm of snow surface. The surface area for 50 μm of snow per unit volume air is $\approx$500 cm^2/g $\times$ 0.4 g/cm^3 $\times$ 50 μm = 1 cm^2; $A_c \approx 1$cm^2/1cm^3.